Limits on Neutrino Emission from GRB 221009A from MeV to PeV using the IceCube Neutrino Observatory

R. Abbasi,[17] M. Ackermann,[64] J. Adams,[18] S. Agarwalla,[41] N. Aggarwal,[25] J. A. Aguilar,[12] M. Ahlers,[22] J.M. Alameddine,[23] N. M. Amin,[45] K. Andeen,[43] G. Anton,[26] C. Argüelles,[14] Y. Ashida,[41] S. Athanasiadou,[64] S. N. Axani,[45] X. Bai,[51] A. Balagopal V.,[41] M. Baricevic,[41] S. W. Barwick,[30] V. Basu,[41] R. Bay,[8] J. J. Beatty,[20,21] K.-H. Becker,[63] J. Becker Tjus,[11,*] J. Beise,[62] C. Bellenghi,[27] S. BenZvi,[53] D. Berley,[19] E. Bernardini,[49] D. Z. Besson,[36] G. Binder,[8,9] D. Bindig,[63] E. Blaufuss,[19] S. Blot,[64] F. Bontempo,[31] J. Y. Book,[14] J. Borowka,[1] C. Boscolo Meneguolo,[49] S. Böser,[42] O. Botner,[62] J. Böttcher,[1] E. Bourbeau,[22] J. Braun,[41] B. Brinson,[6] J. Brostean-Kaiser,[64] R. T. Burley,[2] R. S. Busse,[44] M. A. Campana,[50] K. Carloni,[14] E. G. Carnie-Bronca,[2] C. Chen,[6] Z. Chen,[56] D. Chirkin,[41] S. Choi,[57] B. A. Clark,[24] L. Classen,[44] A. Coleman,[62] G. H. Collin,[15] A. Connolly,[20,21] J. M. Conrad,[15] P. Coppin,[13] P. Correa,[13] S. Countryman,[47] D. F. Cowen,[60,61] C. Dappen,[1] P. Dave,[6] C. De Clercq,[13] J. J. DeLaunay,[59] D. Delgado López,[14] H. Dembinski,[45] K. Deoskar,[55] A. Desai,[41] P. Desiati,[41] K. D. de Vries,[13] G. de Wasseige,[38] T. DeYoung,[24] A. Diaz,[15] J. C. Díaz-Vélez,[41] M. Dittmer,[44] A. Domi,[26] H. Dujmovic,[31] M. A. DuVernois,[41] T. Ehrhardt,[42] P. Eller,[27] R. Engel,[31,32] H. Erpenbeck,[1] J. Evans,[19] P. A. Evenson,[45] K. L. Fan,[19] A. R. Fazely,[7] A. Fedynitch,[58] N. Feigl,[10] S. Fiedlschuster,[26] C. Finley,[55] L. Fischer,[64] D. Fox,[60] A. Franckowiak,[11] E. Friedman,[19] A. Fritz,[42] P. Fürst,[1] T. K. Gaisser,[45] J. Gallagher,[40] E. Ganster,[1] A. Garcia,[14] S. Garrappa,[64] L. Gerhardt,[9] A. Ghadimi,[59] C. Glaser,[62] T. Glauch,[27] T. Glüsenkamp,[26,62] N. Goehlke,[32] J. G. Gonzalez,[45] S. Goswami,[59] D. Grant,[24] S. J. Gray,[19] S. Griffin,[41] S. Griswold,[53] C. Günther,[1] P. Gutjahr,[23] C. Haack,[27] A. Hallgren,[62] R. Halliday,[24] L. Halve,[1] F. Halzen,[41] H. Hamdaoui,[56] M. Ha Minh,[27] K. Hanson,[41] J. Hardin,[15,41] A. A. Harnisch,[24] P. Hatch,[33] A. Haungs,[31] K. Helbing,[63] J. Hellrung,[11] F. Henningsen,[27] L. Heuermann,[1] S. Hickford,[63] A. Hidvegi,[55] C. Hill,[16] G. C. Hill,[2] K. D. Hoffman,[19] K. Hoshina,[41,†] W. Hou,[31] T. Huber,[31] K. Hultqvist,[55] M. Hünnefeld,[23] R. Hussain,[41] K. Hymon,[23] S. In,[57] N. Iovine,[12] A. Ishihara,[16] M. Jansson,[55] G. S. Japaridze,[5] M. Jeong,[57] M. Jin,[14] B. J. P. Jones,[4] D. Kang,[31] W. Kang,[57] X. Kang,[50] A. Kappes,[44] D. Kappesser,[42] L. Kardum,[23] T. Karg,[64] M. Karl,[27] A. Karle,[41] U. Katz,[26] M. Kauer,[41] J. L. Kelley,[41] A. Kheirandish,[34,35] K. Kin,[16] J. Kiryluk,[56] S. R. Klein,[8,9] A. Kochocki,[24] R. Koirala,[45] H. Kolanoski,[10] T. Kontrimas,[27] L. Köpke,[42] C. Kopper,[24] D. J. Koskinen,[22] P. Koundal,[31] M. Kovacevich,[50] M. Kowalski,[10,64] T. Kozynets,[22] C. Kruiswijk,[38] E. Krupczak,[24] A. Kumar,[64] E. Kun,[11] N. Kurahashi,[50] N. Lad,[64] C. Lagunas Gualda,[64] M. Lamoureux,[38] M. J. Larson,[19] F. Lauber,[63] J. P. Lazar,[14,41] J. W. Lee,[57] K. Leonard DeHolton,[60,61] A. Leszczyńska,[45] M. Lincetto,[11] Q. R. Liu,[41] M. Liubarska,[25] E. Lohfink,[42] C. Love,[50] C. J. Lozano Mariscal,[44] L. Lu,[41] F. Lucarelli,[28] A. Ludwig,[37] W. Luszczak,[20,21] Y. Lyu,[8,9] W. Y. Ma,[64] J. Madsen,[41] K. B. M. Mahn,[24] Y. Makino,[41] S. Mancina,[41,49] W. Marie Sainte,[41] I. C. Mariş,[12] S. Marka,[47] Z. Marka,[47] M. Marsee,[59] I. Martinez-Soler,[14] R. Maruyama,[46] F. Mayhew,[24] T. McElroy,[25] F. McNally,[39] J. V. Mead,[22] K. Meagher,[41] S. Mechbal,[64] A. Medina,[21] M. Meier,[16] S. Meighen-Berger,[27] Y. Merckx,[13] L. Merten,[11] J. Micallef,[24] D. Mockler,[12] T. Montaruli,[28] R. W. Moore,[25] Y. Morii,[16] R. Morse,[41] M. Moulai,[41] T. Mukherjee,[31] R. Naab,[64] R. Nagai,[16] U. Naumann,[63] J. Necker,[64] M. Neumann,[44] H. Niederhausen,[24] M. U. Nisa,[24] A. Noell,[1] S. C. Nowicki,[24] A. Obertacke Pollmann,[63] M. Oehler,[31] B. Oeyen,[29] A. Olivas,[19] R. Orsoe,[27] J. Osborn,[41] E. O'Sullivan,[62] H. Pandya,[45] N. Park,[33] G. K. Parker,[4] E. N. Paudel,[45] L. Paul,[43] C. Pérez de los Heros,[62] J. Peterson,[41] S. Philippen,[1] S. Pieper,[63] A. Pizzuto,[41] M. Plum,[51] Y. Popovych,[42] M. Prado Rodriguez,[41] B. Pries,[24] R. Procter-Murphy,[19] G. T. Przybylski,[9] C. Raab,[12] J. Rack-Helleis,[42] K. Rawlins,[3] Z. Rechav,[41] A. Rehman,[45] P. Reichherzer,[11] G. Renzi,[12] E. Resconi,[27] S. Reusch,[64] W. Rhode,[23] M. Richman,[50] B. Riedel,[41] E. J. Roberts,[2] S. Robertson,[8,9] S. Rodan,[57] G. Roellinghoff,[57] M. Rongen,[42] C. Rott,[54,57] T. Ruhe,[23] L. Ruohan,[27] D. Ryckbosch,[29] S.Athanasiadou,[64] I. Safa,[14,41] J. Saffer,[32] D. Salazar-Gallegos,[24] P. Sampathkumar,[31] S. E. Sanchez Herrera,[24] A. Sandrock,[23] M. Santander,[59] S. Sarkar,[25] S. Sarkar,[48] J. Savelberg,[1] P. Savina,[41] M. Schaufel,[1] H. Schieler,[31] S. Schindler,[26] B. Schlüter,[44] T. Schmidt,[19] J. Schneider,[26] F. G. Schröder,[31,45] L. Schumacher,[27] G. Schwefer,[1] S. Sclafani,[50] D. Seckel,[45] S. Seunarine,[52] A. Sharma,[62] S. Shefali,[32] N. Shimizu,[16] M. Silva,[41] B. Skrzypek,[14] B. Smithers,[4] R. Snihur,[41] J. Soedingrekso,[23] A. Søgaard,[22] D. Soldin,[32] G. Sommani,[11] C. Spannfellner,[27] G. M. Spiczak,[52] C. Spiering,[64] M. Stamatikos,[21] T. Stanev,[45] R. Stein,[64] T. Stezelberger,[9] T. Stürwald,[63] T. Stuttard,[22] G. W. Sullivan,[19] I. Taboada,[6] S. Ter-Antonyan,[7] W. G. Thompson,[14] J. Thwaites,[41] S. Tilav,[45] K. Tollefson,[24] C. Tönnis,[57] S. Toscano,[12] D. Tosi,[41] A. Trettin,[64] C. F. Tung,[6] R. Turcotte,[31] J. P. Twagirayezu,[24] B. Ty,[41] M. A. Unland Elorrieta,[44] K. Upshaw,[7] N. Valtonen-Mattila,[62] J. Vandenbroucke,[41] N. van Eijndhoven,[13] D. Vannerom,[15] J. van Santen,[64] J. Vara,[44] J. Veitch-Michaelis,[41] M. Venugopal,[31] S. Verpoest,[29] D. Veske,[47] C. Walck,[55] T. B. Watson,[4] C. Weaver,[24] P. Weigel,[15] A. Weindl,[31] J. Weldert,[60,61] C. Wendt,[41] J. Werthebach,[23] M. Weyrauch,[31] N. Whitehorn,[24,37] C. H. Wiebusch,[1] N. Willey,[24] D. R. Williams,[59] M. Wolf,[41] G. Wrede,[26] J. Wulff,[11] X. W. Xu,[7] J. P. Yanez,[25] E. Yildizci,[41] S. Yoshida,[16] F. Yu,[14] S. Yu,[24] T. Yuan,[41] Z. Zhang[56] and P. Zhelnin[14]

(IceCube Collaboration)

[1] *III. Physikalisches Institut, RWTH Aachen University, D-52056 Aachen, Germany*
[2] *Department of Physics, University of Adelaide, Adelaide, 5005, Australia*
[3] *Dept. of Physics and Astronomy, University of Alaska Anchorage, 3211 Providence Dr., Anchorage, AK 99508, USA*
[4] *Dept. of Physics, University of Texas at Arlington, 502 Yates St., Science Hall Rm 108, Box 19059, Arlington, TX 76019, USA*
[5] *CTSPS, Clark-Atlanta University, Atlanta, GA 30314, USA*
[6] *School of Physics and Center for Relativistic Astrophysics, Georgia Institute of Technology, Atlanta, GA 30332, USA*
[7] *Dept. of Physics, Southern University, Baton Rouge, LA 70813, USA*
[8] *Dept. of Physics, University of California, Berkeley, CA 94720, USA*
[9] *Lawrence Berkeley National Laboratory, Berkeley, CA 94720, USA*
[10] *Institut für Physik, Humboldt-Universität zu Berlin, D-12489 Berlin, Germany*
[11] *Fakultät für Physik & Astronomie, Ruhr-Universität Bochum, D-44780 Bochum, Germany*
[12] *Université Libre de Bruxelles, Science Faculty CP230, B-1050 Brussels, Belgium*
[13] *Vrije Universiteit Brussel (VUB), Dienst ELEM, B-1050 Brussels, Belgium*
[14] *Department of Physics and Laboratory for Particle Physics and Cosmology, Harvard University, Cambridge, MA 02138, USA*
[15] *Dept. of Physics, Massachusetts Institute of Technology, Cambridge, MA 02139, USA*
[16] *Dept. of Physics and The International Center for Hadron Astrophysics, Chiba University, Chiba 263-8522, Japan*
[17] *Department of Physics, Loyola University Chicago, Chicago, IL 60660, USA*
[18] *Dept. of Physics and Astronomy, University of Canterbury, Private Bag 4800, Christchurch, New Zealand*
[19] *Dept. of Physics, University of Maryland, College Park, MD 20742, USA*
[20] *Dept. of Astronomy, Ohio State University, Columbus, OH 43210, USA*
[21] *Dept. of Physics and Center for Cosmology and Astro-Particle Physics, Ohio State University, Columbus, OH 43210, USA*
[22] *Niels Bohr Institute, University of Copenhagen, DK-2100 Copenhagen, Denmark*
[23] *Dept. of Physics, TU Dortmund University, D-44221 Dortmund, Germany*
[24] *Dept. of Physics and Astronomy, Michigan State University, East Lansing, MI 48824, USA*
[25] *Dept. of Physics, University of Alberta, Edmonton, Alberta, Canada T6G 2E1*
[26] *Erlangen Centre for Astroparticle Physics, Friedrich-Alexander-Universität Erlangen-Nürnberg, D-91058 Erlangen, Germany*
[27] *Physik-department, Technische Universität München, D-85748 Garching, Germany*
[28] *Département de physique nucléaire et corpusculaire, Université de Genève, CH-1211 Genève, Switzerland*
[29] *Dept. of Physics and Astronomy, University of Gent, B-9000 Gent, Belgium*
[30] *Dept. of Physics and Astronomy, University of California, Irvine, CA 92697, USA*
[31] *Karlsruhe Institute of Technology, Institute for Astroparticle Physics, D-76021 Karlsruhe, Germany*
[32] *Karlsruhe Institute of Technology, Institute of Experimental Particle Physics, D-76021 Karlsruhe, Germany*
[33] *Dept. of Physics, Engineering Physics, and Astronomy, Queen's University, Kingston, ON K7L 3N6, Canada*
[34] *Department of Physics & Astronomy, University of Nevada, Las Vegas, NV, 89154, USA*
[35] *Nevada Center for Astrophysics, University of Nevada, Las Vegas, NV 89154, USA*
[36] *Dept. of Physics and Astronomy, University of Kansas, Lawrence, KS 66045, USA*
[37] *Department of Physics and Astronomy, UCLA, Los Angeles, CA 90095, USA*
[38] *Centre for Cosmology, Particle Physics and Phenomenology - CP3, Université catholique de Louvain, Louvain-la-Neuve, Belgium*
[39] *Department of Physics, Mercer University, Macon, GA 31207-0001, USA*
[40] *Dept. of Astronomy, University of Wisconsin–Madison, Madison, WI 53706, USA*
[41] *Dept. of Physics and Wisconsin IceCube Particle Astrophysics Center, University of Wisconsin–Madison, Madison, WI 53706, USA*
[42] *Institute of Physics, University of Mainz, Staudinger Weg 7, D-55099 Mainz, Germany*
[43] *Department of Physics, Marquette University, Milwaukee, WI, 53201, USA*
[44] *Institut für Kernphysik, Westfälische Wilhelms-Universität Münster, D-48149 Münster, Germany*
[45] *Bartol Research Institute and Dept. of Physics and Astronomy, University of Delaware, Newark, DE 19716, USA*
[46] *Dept. of Physics, Yale University, New Haven, CT 06520, USA*
[47] *Columbia Astrophysics and Nevis Laboratories, Columbia University, New York, NY 10027, USA*
[48] *Dept. of Physics, University of Oxford, Parks Road, Oxford OX1 3PU, UK*
[49] *Dipartimento di Fisica e Astronomia Galileo Galilei, Università Degli Studi di Padova, 35122 Padova PD, Italy*
[50] *Dept. of Physics, Drexel University, 3141 Chestnut Street, Philadelphia, PA 19104, USA*
[51] *Physics Department, South Dakota School of Mines and Technology, Rapid City, SD 57701, USA*
[52] *Dept. of Physics, University of Wisconsin, River Falls, WI 54022, USA*
[53] *Dept. of Physics and Astronomy, University of Rochester, Rochester, NY 14627, USA*
[54] *Department of Physics and Astronomy, University of Utah, Salt Lake City, UT 84112, USA*
[55] *Oskar Klein Centre and Dept. of Physics, Stockholm University, SE-10691 Stockholm, Sweden*
[56] *Dept. of Physics and Astronomy, Stony Brook University, Stony Brook, NY 11794-3800, USA*
[57] *Dept. of Physics, Sungkyunkwan University, Suwon 16419, Korea*

[58]*Institute of Physics, Academia Sinica, Taipei, 11529, Taiwan*
[59]*Dept. of Physics and Astronomy, University of Alabama, Tuscaloosa, AL 35487, USA*
[60]*Dept. of Astronomy and Astrophysics, Pennsylvania State University, University Park, PA 16802, USA*
[61]*Dept. of Physics, Pennsylvania State University, University Park, PA 16802, USA*
[62]*Dept. of Physics and Astronomy, Uppsala University, Box 516, S-75120 Uppsala, Sweden*
[63]*Dept. of Physics, University of Wuppertal, D-42119 Wuppertal, Germany*
[64]*Deutsches Elektronen-Synchrotron DESY, Platanenallee 6, 15738 Zeuthen, Germany*

(Dated: February 10, 2023)

ABSTRACT

Gamma-ray bursts (GRBs) have long been considered a possible source of high-energy neutrinos. While no correlations have yet been detected between high-energy neutrinos and GRBs, the recent observation of GRB 221009A — the brightest GRB observed by Fermi-GBM to date and the first one to be observed above an energy of 10 TeV — provides a unique opportunity to test for hadronic emission. In this paper, we leverage the wide energy range of the IceCube Neutrino Observatory to search for neutrinos from GRB 221009A. We find no significant deviation from background expectation across event samples ranging from MeV to PeV energies, placing stringent upper limits on the neutrino emission from this source.

Keywords: Neutrino telescopes – Gamma-ray bursts – Particle astrophysics

1. INTRODUCTION

On October 9th 2022 at 13:16:59.99 UT, the Gamma-ray Burst Monitor (GBM) onboard the Fermi satellite triggered and located the exceptionally bright long-duration Gamma-Ray Burst GRB 221009A (Veres et al. 2022; Lesage et al. 2022). This source was also observed by Swift (Palmer et al. 2022; Kennea et al. 2022), Fermi-LAT (Bissaldi et al. 2022), INTEGRAL (SPI-ACS), Konus-Wind, and triangulated by IPN (Svinkin et al. 2022). A highlight among the many multi-wavelength and multi-messenger follow-up searches[‡] of GRB 221009A has been the first detection of γ-rays above an energy of 10 TeV from a GRB as observed by LHAASO (Racusin et al. 2022).

The GBM light curve consists of an initial 17 s long pulse after the GBM trigger (T0), followed by an extraordinarily bright episode starting 221.1 s after T0. The duration (T90) that contains the central 90% of emission from the GRB has a length of (325.8 ± 6.8) s. Given that this GRB saturated the Fermi-GBM instrument, it is possible that this is an over-estimation of the T90. The time-integrated energy flux in the range 10–1000 keV is reported as $(2.912 \pm 0.001) \times 10^{-2}\,\mathrm{erg\,cm^{-2}}$ with a 1.024 s peak photon flux at the level of $(2385 \pm 3)\,\mathrm{cm^{-2}\,s^{-1}}$, making this the most fluent and intense GRB detected by Fermi-GBM (Lesage et al. 2022).

The GRB was also localized using measurements from the Swift Observatory at right ascension $\alpha = 288.2645°$ and declination $\delta = +19.7735°$. The 90% containment of this measurement, as provided by Swift, is 0.61 arcseconds (Palmer et al. 2022). The redshift $z \simeq 0.151$ of the GRB has been inferred from afterglow emission observed with X-SHOOTER of the Very Large Telescope 11.55 hr after T0 (de Ugarte Postigo et al. 2022) corresponding to a luminosity distance of about $D_L \simeq 740$ Mpc (Workman et al. 2022).

Long-duration GRBs are triggered by the death of massive stars. The gravitational and/or magnetic energy that is released in these events is the principal power for the observed bright γ-ray display and has long been speculated to facilitate cosmic ray acceleration (Waxman 1995; Vietri 1995). The interaction of these cosmic rays with ambient radiation and/or matter could yield broadband neutrino emission that, depending on the mechanism, can even precede the electromagnetic emission. The IceCube Observatory has already reported upper limits on neutrino emission of GRB 221009A from a Fast Response Analysis (Thwaites et al. 2022) searching for TeV–PeV neutrino emission in the periods $[\mathrm{T0} - 1\,\mathrm{hr}, \mathrm{T0} + 2\,\mathrm{hr}]$ and $\mathrm{T0} \pm 1$d. An independent search by the KM3NeT Observatory did not find significant neutrino emission in the period $[\mathrm{T0} - 50\,\mathrm{s}, \mathrm{T0} + 5000\,\mathrm{s}]$ either (Dornic et al. 2022).

In this Letter, we report the results of four searches for neutrino emission coincident with GRB 221009A using data collected with the IceCube Observatory. These searches cover complementary energy ranges from few MeV up to the PeV scale, probing neutrino emission from the burst core to high-energy neutrinos produced in external shocks during the GRB.

2. NEUTRINOS FROM GAMMA-RAY BURSTS

One of the leading models for the GRB prompt emission involves a hot and dense plasma ("fireball") that is initially opaque to radiation and expands under its pressure. The ki-

[*] also at Department of Space, Earth and Environment, Chalmers University of Technology, 412 96 Gothenburg, Sweden

[†] also at Earthquake Research Institute, University of Tokyo, Bunkyo, Tokyo 113-0032, Japan

[‡] see https://gcn.gsfc.nasa.gov/ & http://www.astronomerstelegram.org/

netic energy of the resulting highly-relativistic outflow is dissipated via internal shocks, that are expected to form from variations of the bulk Lorentz factor (Rees & Meszaros 1994; Daigne & Mochkovitch 1998; Kobayashi et al. 1997), or via magnetic reconnection in Poynting-flux dominated outflows (Meszaros & Rees 1997). In both cases, electrons are accelerated and produce the bright γ-ray prompt display via synchrotron emission in magnetic fields.

Protons or heavier nuclei entrained in the outflow can also be accelerated by these mechanisms and produce high-energy TeV-PeV neutrinos on collisions with background photons (Waxman & Bahcall 1997; Becker et al. 2006; Murase & Nagataki 2006; Hummer et al. 2012; Bustamante et al. 2015; Biehl et al. 2018; Pitik et al. 2021; Ai & Gao 2022; Liu et al. 2022; Rudolph et al. 2022). Prior to the prompt emission, internal collisions of protons and neutrons below the photosphere have been considered as a source of GeV neutrino emission (Murase et al. 2013; Bahcall & Meszaros 2000; Bartos et al. 2013; Murase et al. 2022). Furthermore, reverse shocks that form during the afterglow phase have been considered sites for efficient cosmic ray acceleration and would yield extremely-high energy neutrinos in the EeV energy range from interactions with optical–UV photons (Waxman & Bahcall 2000; Murase 2007; Thomas et al. 2017; Murase et al. 2022; Zhang et al. 2022). Detection of these neutrinos would be a compelling indicator of (ultra-)high-energy cosmic ray acceleration in gamma-ray bursts.

Gamma-ray bursts could also be promising sites of production of thermal neutrino distributions through different mechanisms; for example, in the standard core-collapse processes, where neutrinos would arrive before the shock break out (Kistler et al. 2013). Neutrino-dominated accretion flows (Liu et al. 2017; Qi et al. 2022) could form in the case of a supernova with jets, producing neutrinos in the MeV energy range that would arrive either prior to the gamma-ray burst (Wang & Meszaros 2007; Wei et al. 2019; Liu et al. 2016), or during the gamma emission (Liu et al. 2016). Finally, the fireball could also be a potential site of neutrino emission with thermal spectra (Halzen & Jaczko 1996), where these neutrinos are predicted to arrive shortly before the photons in a millisecond burst.

Which (if any) of these mechanisms leads to detectable neutrino emission is uncertain, so it is imperative to consider different time windows and energy spectra of GRB neutrino emission in dedicated searches. Previous searches of high-energy neutrino emission carried out by IceCube have so far yielded upper limits which imposed constraints on optimistic neutrino emission models (Abbasi et al. 2009a, 2012a; Aartsen et al. 2015, 2016a; Abbott et al. 2017; Aartsen et al. 2017a; Abbasi et al. 2022a).

3. THE ICECUBE OBSERVATORY

The IceCube Observatory (Aartsen et al. 2017b) is a multi-component facility located at the geographic South Pole. Its main component consists of an in-ice array that utilizes one cubic kilometer of the deep ultra-clear glacial ice as its detector medium. The fiducial volume is instrumented with 5,160 Digital Optical Modules (DOMs) (Abbasi et al. 2009b), each hosting one downward-facing photomultiplier tube (PMT), that register the Cherenkov light emitted by relativistic charged particles passing through the detector (Abbasi et al. 2010). The DOMs are distributed on 86 read-out and support cables ("strings") and are deployed between 1.45 km and 2.45 km below the surface. Most strings follow a triangular grid with a width of 125 m, evenly spaced over the volume.

Eight strings are placed in the centre of the array and are instrumented with a denser DOM spacing and typical inter-string separation of 55 m. They are equipped with PMTs with 35% higher quantum efficiency. These strings, along with the nearest layer of the surrounding standard strings, form the DeepCore low-energy sub-array (Abbasi et al. 2012b). While the original IceCube array has a neutrino energy threshold of about 100 GeV, the addition of the denser infill lowers the energy threshold to about 1 GeV. An additional component of IceCube is the surface air shower array, IceTop (Abbasi et al. 2013), whose data were not used in the analyses presented in this Letter.

Neutrino interactions with matter in the vicinity of the in-ice array create energetic charged particles that are visible via Cherenkov emission. Several triggers are active in IceCube that are designed for the selection of these and other interesting physics events. The principal challenges of astrophysical neutrino observations with IceCube are the large background generated by cosmic ray interactions in the atmosphere and reconstruction of neutrino direction. The better the direction of the neutrino is known, the more background from directions not compatible with the gamma-ray burst can be reduced. At high energies ($\gtrsim$ 100 GeV), enough light is deposited, in particular by energetic muons that are individually reconstructable in both direction and energy, to provide half-degree typical angular resolution. At lower energies ($\sim$ 10–100 GeV), only enough light is collected to reconstruct directions within uncertainties of several to tens of degrees, forcing higher reliance on time correlations with the GRB to reject background. At the lowest energies ($\lesssim$ 10 GeV), individual neutrino interactions are not reconstructable, forcing a complete reliance on timing information. The analyses described in the following section search for neutrinos of a wide variety of energies from astrophysical transients, with a different strategy for each energy range.

4. ANALYSES AND RESULTS

In the following, we summarize the methodology and results of four complementary IceCube analyses of neutrino emission of GRB 221009A. Three of these are based on neutrino event samples that have been developed for previous IceCube analyses: the Gamma-ray Follow-Up (GFU) sample has been optimized for IceCube's real-time program (Aartsen et al. 2016b); the GeV Reconstructed Events with Containment for Oscillations (GRECO) sample was originally developed for oscillation studies with atmospheric neutrinos (Aartsen et al. 2019) and has since been used for low-energy neu-

Table 1. Models for the time-integrated neutrino flux $F(E)$ and energy ranges probed by different datasets. While the analyses based on GFU, GRECO and ELOWEN test broad power-law fluxes the analysis based on SNDAQ probes peaked quasi-thermal fluxes motivated by core-collapse supernovae.

Dataset	Time-Integrated Neutrino Flux Model		
	Power-law : $F(E) \propto E^{-\gamma}$ for $E_{\rm min} \leq E \leq E_{\rm max}$		
	γ	$E_{\rm min}$	$E_{\rm max}$
GFU*	1.5	6.8 TeV	9.9 PeV
	2.0	0.83 TeV	0.96 PeV
	2.5	0.23 TeV	0.086 PeV
	3.0	0.13 TeV	0.013 PeV
GRECO*	1.5	40 GeV	1.5 TeV
	2.0	26 GeV	1.2 TeV
	2.5	15 GeV	0.70 TeV
	3.0	11 GeV	0.35 TeV
ELOWEN	2.0 – 3.0	0.5 GeV	5.0 GeV
	Quasi-thermal : $F_{\bar{\nu}_e}(E) \propto E^2 \exp(-3E/\langle E\rangle)$		
SNDAQ	$E \simeq \langle E\rangle \simeq (10-20)\,{\rm MeV}$		

NOTE— *Central 90% energy range depends on spectral index γ.

trino transients (GRECO Astronomy) (Abbasi et al. 2022b); the Extremely Low-Energy (ELOWEN) event sample was developed for the search of low-energy neutrino emission during solar flares (Abbasi et al. 2021a). In addition, IceCube is able to observe a significant burst of MeV neutrinos through an increased level of single photon hit rates in DOMs across the entire detector. This search is based on a real-time data stream called the Supernova Data Acquisition (SNDAQ) that was developed to detect MeV neutrinos from supernovae (Abbasi et al. 2011).

Table 1 summarizes the test hypotheses for the time-integrated neutrino flux $F(E) \equiv {\rm d}^2N/{\rm d}E/{\rm d}A$ (neutrinos per area A and energy E) and corresponding neutrino energy scales accessible by these different datasets. For the GFU and GRECO datasets the energy interval $[E_{\rm min}, E_{\rm max}]$ corresponds to the central 90% energy range of predicted events for a power-law emission with spectral index γ at the location of GRB 221009A. This table shows the wide MeV–PeV bandwidth covered in the following analyses.

4.1. *Fast Response Analysis: > 100 GeV*

The Fast Response Analysis (FRA) (Abbasi et al. 2021b, 2022c) is a framework established to rapidly follow up interesting transients or multi-messenger events in real time with the IceCube Neutrino Observatory. The FRA requires a real-time data stream, with low-latency access to data from the South Pole, in order to follow up interesting transients in real-time. This GFU sample uses events triggered by causally connected single-photon hits on eight or more neighbouring IceCube DOMs and employs a faster event reconstruction at the expense of some angular resolution available for offline reconstructions (Aartsen et al. 2016b). At final filter level, the stream has an all-sky rate that varies between approximately 6 and 7 mHz due to seasonal variations (Abbasi et al. 2021b).

The FRA uses an unbinned maximum-likelihood method to identify significant neutrino emission following an E^{-2} spectrum on top of background events. The method has been used in other searches for short-timescale neutrino emission from potential sources (Aartsen et al. 2020; Abbasi et al. 2022d,a). We initiated an FRA of GRB 221009A in response to the observations reported by Swift and Fermi-GBM using the time windows *(a)* [T0 − 1 hr , T0 + 2 hr] (3 hours in total) and *(b)* T0 ± 1 d (2 days in total) to cover extended emission periods before and after the Fermi-GBM trigger, as summarized in Thwaites et al. (2022).

In addition to this initial real-time FRA, we also searched for neutrino emission using the same data sample for an extended set of time windows following the method of a previous archival search for neutrinos coincident with GRBs (Abbasi et al. 2022a). This analysis used three time windows in order to search for neutrinos *(c)* during the T90 phase as given by Fermi-GBM, *(d)* during the period [T0 − 200 s , T0 + 2000 s] to include times corresponding to the high energy photons observed by LHAASO (Racusin et al. 2022) as well as potential precursor emission, and *(e)* during the extended period [T0 − 1 d , T0 + 14 d] covering precursor-to-afterglow emission. We scanned over a circle of radius of 1°, centered on the location of GRB 221009A in order to find the location with highest significance, which is consistent with the previous method. Both these analysis assumed an E^{-2} spectrum as in the initial FRA.

None of these analyses — the initial FRA and its application to an extended set of time-windows — found indications for neutrino emission above background expectations, with p-values being close to 1. These results allow us to set upper limits on the energy-scaled time-integrated neutrino flux, $E^2F(E)$, which are summarized in Tab. 2 at a reference energy $E_0 = 100\,{\rm TeV}$. In the case of the standard FRA time windows of 3 hours and 2 days, we provide upper limits for four different power-law indices γ based on Monte-Carlo injections following $F(E) \propto E^{-\gamma}$.

Figure 1 shows the upper limits on the time-integrated neutrino flux for the T90 phase and the time window [T0 − 1 hr , T0 + 2 hr]. These upper limits can be translated into limits on the differential isotropic-equivalent energy ${\rm d}\mathcal{E}_{\rm iso}/{\rm d}E$ of GRB 221009A at redshift z and luminosity distance D_L via the relation $E^2F(E) = E{\rm d}\mathcal{E}_{\rm iso}/{\rm d}E \times (1+z)/(4\pi D_L^2)$. This quantity is indicated by the right axis in Fig. 1.

4.2. *GRECO Astronomy Analysis: 10–1000 GeV*

This analysis focuses on the low-energy GRECO Astronomy dataset, which is optimized for neutrinos between

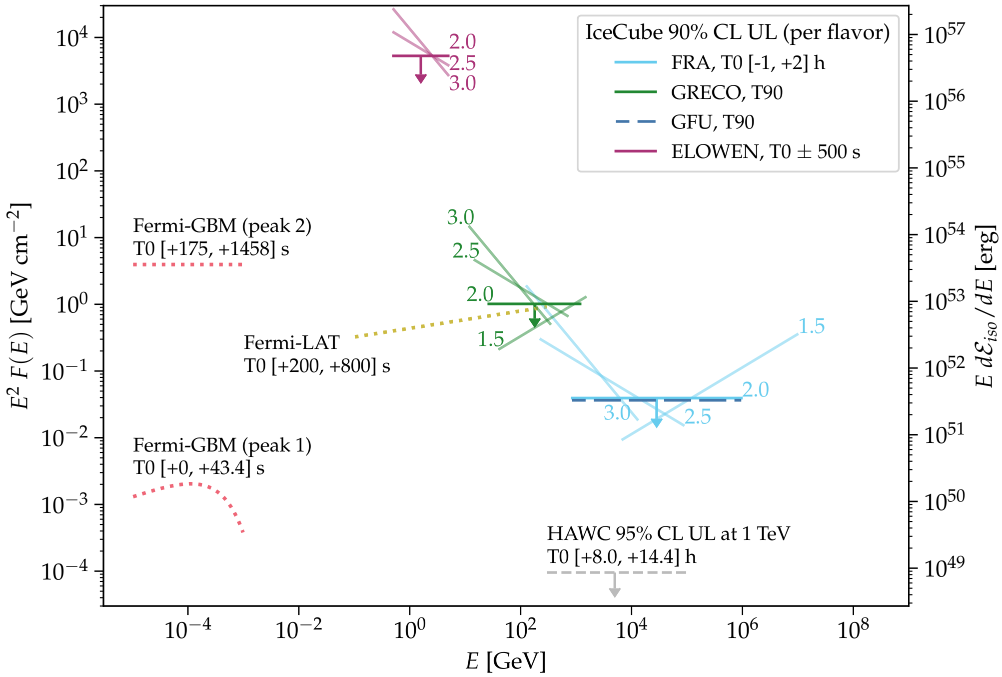

Figure 1. Gamma-ray observations and upper limits on the time-integrated neutrino flux of GRB 221009A. We show the γ-ray observations from Fermi-GBM (Lesage et al. 2022) and Fermi-LAT (Bissaldi et al. 2022) as well as upper limits from HAWC (Ayala et al. 2022). The Fermi-GBM result covering the prompt phase ("peak 2") had no reported spectral fit so it is shown here at $\gamma = 2.0$ for visualization purposes. The upper limits on the time-integrated neutrino flux are shown for various spectral indices as indicated by the numbers. The right axis shows the differential isotropic equivalent energy $d\mathcal{E}_{\rm iso}/dE$.

10 GeV and 1 TeV (Abbasi et al. 2022e). This sample is based on events with at least three coincident hits in DeepCore DOMs and has an average event rate of about 4 mHz at final filter level (Aartsen et al. 2019). In order to test for neutrino emission from GRB 221009A, we use an extended unbinned maximum-likelihood outlined in Abbasi et al. (2022a) combined with a spatial prior to account for the source localization uncertainty. The signal hypothesis assumes an $E^{-2.5}$ neutrino spectrum with equal contributions from all flavors.

To account for the fact that angular uncertainties for the low-energy events used in the GRECO Astronomy dataset are relatively large, a Kent distribution (Kent 1982) is assumed for the spatial likelihood. The localization prior is a 1° radius top-hat distribution centered at the localization provided by Swift. This is done for computational reasons and the size of the prior does not affect the result given that angular uncertainties used in GRECO Astronomy are relatively large.

The analysis of GRB 221009A focused on two time windows, matching those of other analyses at different energy ranges. We searched for neutrino emission (c) coincident with the central 90% emission from the GRB as reported as the T90 phase by Fermi-GBM and (d) the 2,200 second window [T0 − 200 s , T0 + 2000 s] including potential precursor emission and coincidences with high energy photons observed by LHAASO. Though even longer time windows are desirable, too, this is prevented by computational constraints.

We did not find significant deviations from a background distribution in either of the two time windows, with p-values being close to 1 in this analysis. The corresponding upper limits on the energy-scaled time-integrated neutrino flux, $E^2F(E)$, at a reference energy of $E_0 = 1$ TeV for each time window and four different spectral indices can be found in Tab. 2. Similar to the previous analysis, we provide upper limits for different power-law indices γ derived from the corresponding Monte-Carlo injections. Figure 1 shows the upper limits on the time-integrated neutrino flux for the T90 phase.

4.3. *ELOWEN Analysis: 0.5–5 GeV*

The selection of events below 10 GeV at IceCube is challenging due to the presence of large atmospheric backgrounds and the lack of directional reconstruction in this energy range. However, relying on temporal coincidence makes it possible to search for potential neutrino emission in the GeV energy range. Here, we follow the methods used in a previous analysis in this energy range (Abbasi et al. 2021c), which are briefly summarized here. Two short time windows were chosen based on archival electromagnetic data from GRBs (Baret et al. 2011) while minimizing the impact of the background for our neutrino search: *(f)* a 1,000 second window T0 ± 500 s centered on the Fermi-GBM trigger and *(d)* the 2,200 second window [T0 − 200 s , T0 + 2000 s] also used in other analyses.

Because of the reliance on timing in this analysis, we require a precise model of the background event rate as the key component of the search. To determine this, we examined a large number of time windows of the same lengths during

Table 2. Upper limits (UL) on the time-integrated neutrino flux of GRB 221009A for the different time windows discussed in section 4 referenced by their inline text indices. The three analyses based on GFU, GRECO and ELOWEN assume a per-flavor time-integrated power-law flux $F(E) \propto E^{-\gamma}$ with variable spectral index γ. The results are given for the energy-scaled time-integrated per-flavor neutrino flux, $E^2F(E)$, at a reference energy E_0 depending on the dataset. The analysis based on the SNDAQ assumes an electron anti-neutrino spectrum following a quasi-thermal spectrum peaked at $\langle E \rangle = 15$ MeV. Results are shown for the total and peak time-integrated $\bar{\nu}_e$ flux.

Dataset	Time Window & Index		90% C.L. Upper Limits (ULs) on the Time-integrated Neutrino Flux $F(E)$				
			Power-law $F(E) \propto E^{-\gamma}$: per-flavor ULs show $E^2F(E)$ [GeV cm^{-2}] at E_0				
			E_0	$\gamma = 1.5$	$\gamma = 2.0$	$\gamma = 2.5$	$\gamma = 3.0$
GFU	[T0 − 1 hr , T0 + 2 hr]	*(a)*	100 TeV	0.0359	0.0393*	0.0143	0.00240
	T0 ± 1 d	*(b)*		0.0370	0.0410*	0.0176	0.00345
	T90 phase	*(c)*		⋯	0.0364	⋯	⋯
	[T0 − 200 s , T0 + 2000 s]	*(d)*		⋯	0.0369	⋯	⋯
	[T0 − 1 d , T0 + 14 d]	*(e)*		⋯	0.0471	⋯	⋯
GRECO	T90 phase	*(c)*	1 TeV	1.052	1.015	0.561	0.174
	[T0 − 200 s , T0 + 2000 s]	*(d)*		1.387	1.338	0.740	0.229
ELOWEN	T0 ± 500 s	*(f)*	1 GeV	⋯	5.3×10^3	8.7×10^3	1.4×10^4
	[T0 − 200 s , T0 + 2000 s]	*(d)*		⋯	7.9×10^3	1.3×10^4	2.0×10^4
			Quasi-thermal $F_{\bar{\nu}_e}(E) \propto E^2 \exp(-3E/\langle E \rangle)$: $\bar{\nu}_e$ UL on total and peak flux				
			$\langle E \rangle$	Total $\bar{\nu}_e$ Flux [cm^{-2}]		$E^2F_{\bar{\nu}_e}(E)$ [GeV cm^{-2}] at $\langle E \rangle$	
SNDAQ	[T0 − 100 s , T0]	*(g)*	15 MeV	7.98×10^8		8.05×10^6	
	[T0 − 1 s , T0]	*(h)*		1.81×10^9		1.82×10^7	
	[T0 , T0 + 17 s]	*(i)*		8.00×10^8		8.07×10^6	
	[T0 + 18 s , T0 + 174 s]	*(j)*		3.08×10^8		3.11×10^6	
	[T0 + 174 s , T0 + 175 s]	*(k)*		1.35×10^9		1.36×10^7	
	[T0 + 175 s , T0 + 547 s]	*(l)*		4.00×10^8		4.03×10^6	

NOTE— *Values corresponding to the real-time FRA results published in Thwaites et al. (2022).

time periods where no transient events were detected (GRBs, gravitational waves, or — for the longer window — classical novae). The rates in these windows, as well as in the 8-hour period immediately before the GRB, were statistically compatible with the expected background data rate of 0.2 Hz, validating our background model.

Like GRECO, the dataset is based on events with at least three coincident hits in DeepCore DOMs. The filtering process for ELOWEN, which is explained in more detail in Abbasi et al. (2021a), keeps 40% of the initial sample of neutrinos following an E^{-2} spectrum from 0.5 GeV to 5 GeV, simulated with GENIE 2.8.6 (Andreopoulos et al. 2010), while reducing the background from atmospheric muons and detector noise (Abbasi et al. 2010, 2009b; Larson 2013) by >99.9%.

The significance of any excess observed during the on-time phase can then be calculated by comparison to the off-time phase with the methods described in Li & Ma (1983). None of the tested time windows showed indications for neutrino emission in the $0.5 - 5$ GeV energy range; we find p-values larger than 0.7. The corresponding upper limits on the energy-scaled time-integrated neutrino flux, $E^2F(E)$, at a reference energy of $E_0 = 1$ GeV can be found in Tab. 2 for three different spectral indices of the simulated power-law spectrum. Figure 1 shows the upper limits on the time-integrated flux for the 1,000 second time window.

4.4. *MeV Neutrino Burst Analysis: < 1 GeV*

IceCube can observe a significant burst of sub-GeV neutrinos through an increased level of single photon hit rates on the PMTs across the entire detector, predominantly from the reaction $\bar{\nu}_e + p \rightarrow e^+ + n$, compared to the uncorrelated single-PMT noise rate at the level of about 0.5 kHz (Abbasi et al. 2010). In this analysis, we use the SNDAQ data stream designed for the detection of supernovae (Abbasi et al. 2011) to search for MeV neutrinos from GRB 221009A. We divide the search into six time windows covering from 100 s prior to T0 up to the end of T90 for a total of 647 seconds. These time windows, shown at the bottom of Tab. 2, were selected to search for MeV neutrino emission *(g)* 100 s and *(h)* 1 s prior to the precursor, *(i)* during the precursor phase, *(j)* during the phase between precursor and prompt emission, *(k)* 1 s prior to the prompt phase, and *(l)* the T90 phase. To find the excess rates in the different time windows, we use a sliding 1 s search window to identify the highest rate during each of the longer time periods. For the shortest time windows spanning 1 s, we instead use a 0.5 s sliding search window.

To calculate the significance of the observed number of hits at the time of the GRB compared to what is expected from the background, we repeat the search method described above for each time window on two weeks of off-time data: one week prior to the GRB and one week after. The upper limit on the observed hits is obtained using the method of Feldman & Cousins (1998) for a 90% C.L. These hits upper limits are then used to obtain an upper limit on the time-integrated flux through A Supernova Test Routine for IceCube Analysis (ASTERIA) (Griswold et al. 2020). ASTERIA is a fast supernova neutrino simulation designed to model the detector response for IceCube.

The neutrino spectra of core-collapse supernovae are expected to evolve in time. For simplicity, all tested time windows in this analysis assume the emission of electron antineutrinos ($\bar{\nu}_e$) following a generic quasi-thermal spectrum inferred from simulations of core-collapse supernovae (Keil et al. 2003) approximated as a Maxwell-Boltzmann distribution $F_{\bar{\nu}_e}(E) \propto E^2 \exp(-3E/\langle E\rangle)$ with mean energy of $\langle E\rangle = 15\,\mathrm{MeV}$ (Tamborra et al. 2012). Since the on-time data is consistent with the background for all six time windows ($p > 0.3$), we set 90% C.L. upper limit for the total time-integrated flux of electron antineutrinos and the energy-scaled time-integrated flux, $E^2 F_{\bar{\nu}_e}(E)$, at the peak $\langle E\rangle$ for each time window in Tab. 2.

5. CONCLUSIONS

Our searches did not find significant neutrino emission in an energy range from MeV to PeV, before, during, or after the electromagnetic emission, resulting in upper limits on the time-integrated neutrino flux of GRB 221009A. These upper limits allow constraints on neutrino emission models from this source, as discussed by Murase et al. (2022), Liu et al. (2022) or Rudolph et al. (2022). Previous IceCube searches for the joint neutrino emission of GRBs showed that high-energy neutrino emission during the prompt phase (or during 10^4 s) of GRBs is limited to $\leq$ 1% (or $\leq$ 24%) of the high-energy diffuse neutrino flux observed by IceCube (Abbasi et al. 2022a).

Future upgrades and proposed extensions of IceCube could provide a crucial step towards neutrino detection from GRBs. The IceCube-Upgrade (Ishihara 2021) will enhance the detection of 1-10 GeV neutrino events with respect to the GRECO Astronomy and ELOWEN samples and will improve the angular reconstruction above 10 GeV. The proposed multi-component extension IceCube-Gen2 (Aartsen et al. 2021) would significantly increase the sensitivity to high-energy neutrino transients, *e.g.* increasing the observable volume within our Universe by one order of magnitude for TeV–PeV neutrinos compared to IceCube.

ACKNOWLEDGMENTS

The IceCube Collaboration acknowledges Eric Burns for valuable discussions of public Fermi-GBM results. The authors gratefully acknowledge the support from the following agencies and institutions: USA – U.S. National Science Foundation-Office of Polar Programs, U.S. National Science Foundation-Physics Division, U.S. National Science Foundation-EPSCoR, Wisconsin Alumni Research Foundation, Center for High Throughput Computing (CHTC) at the University of Wisconsin–Madison, Open Science Grid (OSG), Advanced Cyberinfrastructure Coordination Ecosystem: Services & Support (ACCESS), Frontera computing project at the Texas Advanced Computing Center, U.S. Department of Energy-National Energy Research Scientific Computing Center, Particle astrophysics research computing center at the University of Maryland, Institute for Cyber-Enabled Research at Michigan State University, and Astroparticle physics computational facility at Marquette University; Belgium – Funds for Scientific Research (FRS-FNRS and FWO), FWO Odysseus and Big Science programmes, and Belgian Federal Science Policy Office (Belspo); Germany – Bundesministerium für Bildung und Forschung (BMBF), Deutsche Forschungsgemeinschaft (DFG), Helmholtz Alliance for Astroparticle Physics (HAP), Initiative and Networking Fund of the Helmholtz Association, Deutsches Elektronen Synchrotron (DESY), and High Performance Computing cluster of the RWTH Aachen; Sweden – Swedish Research Council, Swedish Polar Research Secretariat, Swedish National Infrastructure for Computing (SNIC), and Knut and Alice Wallenberg Foundation; European Union – EGI Advanced Computing for research; Australia – Australian Research Council; Canada – Natural Sciences and Engineering Research Council of Canada, Calcul Québec, Compute Ontario, Canada Foundation for Innovation, WestGrid, and Compute Canada; Denmark – Villum Fonden, Carlsberg Foundation, and European Commission; New Zealand – Marsden Fund; Japan – Japan Society for Promotion of Science (JSPS) and Institute for Global Prominent Research (IGPR) of Chiba University; Korea – National Research Foundation of Korea (NRF); Switzerland – Swiss National Science Foundation (SNSF); United Kingdom – Department of Physics, University of Oxford.

REFERENCES

Aartsen, M. G., et al. 2015, Astrophys. J. Lett., 805, L5

—. 2016a, Astrophys. J., 824, 115

—. 2016b, JINST, 11, P11009

—. 2017a, Astrophys. J., 843, 112

—. 2017b, JINST, 12, P03012

—. 2019, Phys. Rev. D, 99, 032007

—. 2020, Astrophys. J., 890, 111
—. 2021, J. Phys. G, 48, 060501
Abbasi, R., et al. 2009a, Astrophys. J., 701, 1721
—. 2009b, Nucl. Instrum. Meth. A, 601, 294
—. 2010, Nucl. Instrum. Meth. A, 618, 139
—. 2011, Astron. Astrophys., 535, A109
—. 2012a, Nature, 484, 351
—. 2012b, Astropart. Phys., 35, 615
—. 2013, Nucl. Instrum. Meth. A, 700, 188
—. 2021a, Phys. Rev. D, 103, 102001
—. 2021b, Astrophys. J., 910, 4
—. 2021c. https://arxiv.org/abs/2105.13160
—. 2022a, Astrophys. J., 939, 116
—. 2022b, JCAP, 01, 027
—. 2022c. https://arxiv.org/abs/2210.04930
—. 2022d. https://arxiv.org/abs/2208.09532
—. 2022e. https://arxiv.org/abs/2212.06810
Abbott, B. P., et al. 2017, Astrophys. J. Lett., 848, L12
Ai, S., & Gao, H. 2022. https://arxiv.org/abs/2210.14116
Andreopoulos, C., et al. 2010, Nucl. Instrum. Meth. A, 614, 87
Ayala, H., et al. 2022, GCN Circular 32683
Bahcall, J. N., & Meszaros, P. 2000, Phys. Rev. Lett., 85, 1362
Baret, B., et al. 2011, Astropart. Phys., 35, 1
Bartos, I., Beloborodov, A. M., Hurley, K., & Márka, S. 2013, Phys. Rev. Lett., 110, 241101
Becker, J. K., Stamatikos, M., Halzen, F., & Rhode, W. 2006, Astropart. Phys., 25, 118
Biehl, D., Boncioli, D., Fedynitch, A., & Winter, W. 2018, Astron. Astrophys., 611, A101
Bissaldi, E., et al. 2022, GCN Circular 32637
Bustamante, M., Baerwald, P., Murase, K., & Winter, W. 2015, Nature Commun., 6, 6783
Daigne, F., & Mochkovitch, R. 1998, Mon. Not. Roy. Astron. Soc., 296, 275
de Ugarte Postigo, A., et al. 2022, GCN Circular 32648
Dornic, D., et al. 2022, GCN Circular 32741
Feldman, G. J., & Cousins, R. D. 1998, Phys. Rev. D, 57, 3873
Griswold, S., BenZvi, S., Uberoi, N., & Cross, R. 2020
Halzen, F., & Jaczko, G. 1996, Phys. Rev. D, 54, 2779
Hummer, S., Baerwald, P., & Winter, W. 2012, Phys. Rev. Lett., 108, 231101
Ishihara, A. 2021, PoS, ICRC2019, 1031
Keil, M. T., Raffelt, G. G., & Janka, H.-T. 2003, Astrophys. J., 590, 971
Kennea, J., et al. 2022, GCN Circular 32635
Kent, J. T. 1982, J. Roy. Statist. Soc. Ser. B, 44, 71
Kistler, M. D., Haxton, W. C., & Yüksel, H. 2013, Astrophys. J., 778, 81
Kobayashi, S., Piran, T., & Sari, R. 1997, Astrophys. J., 490, 92
Larson, M. 2013, Master's thesis, University of Alabama. https://docushare.icecube.wisc.edu/dsweb/Get/Document-68303/LarsonThesis_final.pdf
Lesage, S., et al. 2022, GCN Circular 32642
Li, T. P., & Ma, Y. Q. 1983, Astrophys. J., 272, 317
Liu, R.-Y., Zhang, H.-M., & Wang, X.-Y. 2022. https://arxiv.org/abs/2211.14200
Liu, T., Gu, W.-M., & Zhang, B. 2017, New Astron. Rev., 79, 1
Liu, T., Zhang, B., Li, Y., Ma, R.-Y., & Xue, L. 2016, Phys. Rev. D, 93, 123004
Meszaros, P., & Rees, M. J. 1997, Astrophys. J. Lett., 482, L29
Murase, K. 2007, Phys. Rev. D, 76, 123001
Murase, K., Kashiyama, K., & Mészáros, P. 2013, Phys. Rev. Lett., 111, 131102
Murase, K., Mukhopadhyay, M., Kheirandish, A., Kimura, S. S., & Fang, K. 2022, Astrophys. J. Lett., 941, L10
Murase, K., & Nagataki, S. 2006, Phys. Rev. D, 73, 063002
Palmer, D., et al. 2022, GCN Circular 32632
Pitik, T., Tamborra, I., & Petropoulou, M. 2021, JCAP, 05, 034
Qi, Y.-Q., Liu, T., Huang, B.-Q., Wei, Y.-F., & Bu, D.-F. 2022, Astrophys. J., 925, 43
Racusin, J., et al. 2022, GCN Circular 32677
Rees, M. J., & Meszaros, P. 1994, Astrophys. J. Lett., 430, L93
Rudolph, A., Petropoulou, M., Winter, W., & Bošnjak, v. 2022. https://arxiv.org/abs/2212.00766
Svinkin, D., et al. 2022, GCN Circular 32641
Tamborra, I., Muller, B., Hudepohl, L., Janka, H.-T., & Raffelt, G. 2012, Phys. Rev. D, 86, 125031
Thomas, J. K., Moharana, R., & Razzaque, S. 2017, Phys. Rev. D, 96, 103004
Thwaites, J., et al. 2022, GCN Circular 32665
Veres, P., et al. 2022, GCN Circular 32636
Vietri, M. 1995, Astrophys. J., 453, 883
Wang, X.-Y., & Meszaros, P. 2007, Astrophys. J., 670, 1247
Waxman, E. 1995, Phys. Rev. Lett., 75, 386
Waxman, E., & Bahcall, J. N. 1997, Phys. Rev. Lett., 78, 2292
—. 2000, Astrophys. J., 541, 707
Wei, Y.-F., Liu, T., & Song, C.-Y. 2019, Astrophys. J., 878, 142
Workman, R. L., et al. 2022, PTEP, 2022, 083C01
Zhang, B. T., Murase, K., Ioka, K., et al. 2022. https://arxiv.org/abs/2211.05754